

# Forecast of Total Real and Reactive Power Losses for Systems under Contingency via Function Fitting Artificial Neural Network

G. G. da Silva, W. P. L. dos Santos, A. de Queiroz, E. Garbelini and A. Bonini Neto

**Abstract--** Technical energy losses in power systems are an inevitable phenomenon that occur due to transformer impedance, conductor resistance, equipment losses, line reactance, and phase imbalance. Minimizing these losses is crucial for system efficiency. This work presents an innovative approach using artificial neural networks (ANN) to obtain complete curves of real and reactive power losses in power systems subjected to contingencies. The distinguishing feature of this methodology lies in the speed with which all curves of the system are obtained, both under normal operating conditions and in contingency situations (simple or severe). The main advantage of using ANN models is their ability to capture the nonlinear characteristics of the system, thus avoiding iterative procedures. The results demonstrated that the ANN performed satisfactorily, with a mean squared error in training below the specified value. For the samples that were not part of the training, the network was able to estimate 99% of the real and reactive power losses within the established range, with residuals around  $10^{-3}$  and an accuracy rate also of approximately 99% between the desired and obtained output.

**Index Terms—** Continuation method, Artificial intelligence, Technical energy losses, Estimation, Loading margin.

## I. NOMENCLATURE

ANN – Artificial Neural Network.  
MLP – Multilayer Perceptron.  
 $Y_{des}$  – Desired Output.  
 $Y_{ob}$  – Obtained Output.  
MSE - Mean Square Error.  
CP – Critical Point.  
CPF - Continuation Power Flow.  
PF - Power Flow.  
EPS - Electric Power Systems.  
LM - Loading Margin.

TL - Transmission Lines.  
ONS - National Electric System Operator.  
WSCC - Western System Coordinating Council.  
 $Pa$  - Total Real Power Losses.  
 $Pr$  - Total Reactive Power Losses.

## II. INTRODUCTION

ELECTRICITY is an essential resource worldwide, with continuity and quality of supply being fundamental to our quality of life [1]. Currently, the increase in demand, combined with the deregulation of the electricity sector and restrictive policies on the construction of new transmission lines and hydroelectric plants, has led power systems (PS) to operate close to their operational limits, i.e., near the critical point (CP). Additionally, the scarcity of rainfall often results in energy rationing, especially in countries like Brazil, where 60% of the demand is met by hydroelectric power [2].

Systems operating close to their limits are more prone to contingencies. In this context, security analysis is crucial to identify contingencies that may impact the system. An electrical system faces numerous contingencies, but few are severe enough to cause instability [3].

Static voltage stability analysis, which involves P-V and Q-V curves to determine the loading margin, is the main tool in contingency studies. Continuation power flow (CPF) with parameterization techniques [4] – [6] is the method used to obtain these curves, allowing for the complete acquisition of P-V curves using the appropriate parameter. It is known that the Western System Coordinating Council [7] requires companies to maintain a safe loading margin of 5% for active power in any single contingency (N-1), and 2.5% for double contingencies (N-2).

These challenges have motivated the electric sector to invest in tools to improve power generation, transmission, and distribution systems [8]. One of these tools is the artificial neural network (ANN) [9] – [11]. Reference [8] shows proposed using a learning algorithm called extreme learning machine (ELM) [15] to predict the voltage stability margin more accurately and efficiently. The model inputs are system operational parameters and loading direction, and the output is the voltage stability margin. Using the algorithm, the mean percentage error was only 3.32%, and the mean error was only 0.0495, results that are satisfactory for practical use.

---

The authors would like to thank the financial support of the Department of Electrical Engineering, UNESP - Bauru.

G. Gonçalves da Silva, Department of Electrical Engineering, FE - UNESP, Bauru- SP - Brasil (e-mail: giovana.goncalves@unesp.br).

W. Prado Leão dos Santos, Department of Biosystems Engineering, FCE - UNESP, Tupã - SP - Brasil (e-mail: alfredo.bonini@unesp.br).

A. de Queiroz, Department of Electrical Engineering, FE - UNESP, Bauru - SP - Brasil (e-mail: alexandre.queiroz@unesp.br).

E. Garbelini, Department of Biosystems Engineering, FCE - UNESP, Tupã - SP - Brasil (e-mail: enio.garb@gmail.com).

A. Bonini Neto, Department of Biosystems Engineering, FCE - UNESP, Tupã - SP - Brasil (e-mail: alfredo.bonini@unesp.br).

Reference [9], a pattern recognition ANN was developed to classify the operating conditions of a power transformer. The network was able to classify the samples with a 98% accuracy rate of the 815 samples presented and with 100% accuracy in validation. Reference [10], an artificial neural network, specifically a Multi-layer Perceptron, was employed to predict total real and reactive power losses in electrical systems in pre-contingency condition only. The results obtained, using datasets from IEEE systems with 14, 30, and 57 buses, showed satisfactory performance, with a mean squared error of around  $10^{-4}$  and a coefficient of determination ( $R^2$ ) of 0.998. In validation with 20% of the data that was not part of the training, the network demonstrated effectiveness, with a mean squared error around  $10^{-3}$ . Reference [11] proposed an ANN (Artificial Neural Networks) approach for obtaining complete P-V curves of power systems subjected to contingencies. Two networks were presented: the MLP (multilayer perceptron) and the RBF (radial basis function). The results showed that the ANN performed well, with a mean squared error (MSE) in training below the specified value. The network was able to estimate 98.4% of the voltage magnitude values within the established range, with residuals around  $10^{-4}$  and a success rate of approximately 98% between the desired and obtained output, with the RBF network performing better than the MLP (Multilayer Perceptron).

Promising results were also found by Aydin and [13], where the ANN reproduced the same results with high accuracy and speed compared to conventional voltage stability calculation methods. The loading parameter and voltage stability margin index were calculated using eight different input variables and fourteen different training functions, allowing the identification of the fastest and most effective training function.

In this context, this work presents an innovative approach compared to the aforementioned studies for obtaining real and reactive power loss curves in pre- and post-contingency scenarios. It is proposed to use artificial neural networks (ANN) to estimate these technical losses and, consequently, the loading margin of a system not only under normal operating conditions but also subjected to simple or severe contingencies.

### III. METHODOLOGY

The system analyzed in this study is the IEEE 14-bus configuration, as illustrated in Fig. 1. The 1890 samples used for training and validation were obtained using the method described in [4]. Each sample consists of 6 data points: 4 input data for the ANN, which include the loading factor  $\lambda$ , the real and reactive power generated at the slack bus ( $P_g^{\text{slack}}$  and  $Q_g^{\text{slack}}$ ), and the branch number (transmission lines or transformers); and 2 output data points, representing the total real and reactive power losses of the system.

The IEEE 14-bus system has 20 branches, as shown in Fig. 1. Ninety samples were generated for each branch removed from the system, representing the applied contingency. Removing branch 1 (r1) from the system results in a severe N-

2 contingency (double contingency), causing a significant reduction in the system's loading margin, as indicated in the results. The other contingencies are classified as simple (N-1). In this study, the symbol N-0 refers to the system without contingency, that is, the pre-contingency P-V curve (r0).

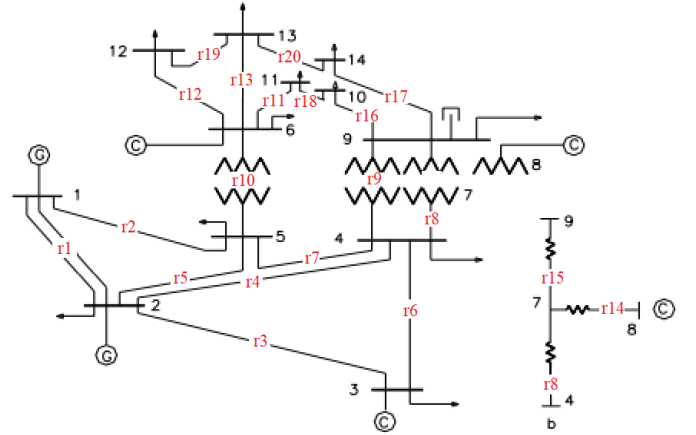


Fig. 1. IEEE 14-bus system with respective branches r.

The Artificial Neural Network (ANN) used was a feedforward multilayer perceptron [14], trained with the backpropagation algorithm [15]. The network structure consists of three layers: an input layer with 4 neurons, a hidden layer with 10 neurons, and an output layer with 2 neurons, as illustrated in Fig. 2. The Matlab® software [16] was employed for both data preparation and results generation.

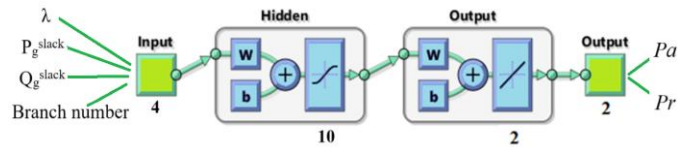


Fig. 2. ANN used in this work.

The value of  $\mathbf{u}_k$  (1) represents the sum of the products of the inputs  $\mathbf{x}$  by their respective weights  $\mathbf{W}$ , plus the bias. The bias increases the degrees of freedom, allowing the neural network to better adapt to the provided knowledge.

$$\mathbf{u}_k = \sum_{i=1}^n \mathbf{x}_i \mathbf{W}_i + \text{bias} \quad (1)$$

After determining the value of  $\mathbf{u}_k$ , it is necessary to calculate the activation function  $\mathbf{f}(\mathbf{u}_k)$  to obtain the output. In this work, the hyperbolic tangent function (2) was used for the hidden layer, while the linear function (3) was employed for the output layer:

$$f(u) = \frac{(1 - e^{-\lambda u})}{(1 + e^{-\lambda u})} \quad (2)$$

where  $\lambda$  is an arbitrary constant representing the inclination of the curve.

$$f(u) = u \quad (3)$$

#### IV. RESULTS

Table 1 and Figs. 3, 4, and 5 present the results of the 1890 samples used for training and validation. The configuration consisted of 1701 samples for training (90%) and 189 samples for validation (10%). Fig. 3(a) shows the mean squared error (MSE) during training and validation. The iterative process was stopped at the 19th iteration when one of the specified values in Table 1 was reached, with a training value of 0.000858 and a CPU time of 2 seconds (Intel(R) Core i7 2.20GHz processor and 16 GB RAM), indicating good training performance of the network. The great advantage of using ANN models is their ability to capture the nonlinear characteristics of the studied system, avoiding iterative procedures. For samples not included in the training phase, i.e., the validation phase, the MSE was 0.0036841. Table 1 also presents the  $R^2$  (correlation) values for the two phases of the network. The  $R^2$  value in the training phase was 0.9994, indicating that the network was well-trained and there was no significant difference between the desired and obtained values in the classification of the 1701 samples (approximately 98% correlation between the output  $Y_{ob}$  and the desired output  $Y_{des}$ ). For the validation phase, the  $R^2$  value was 0.9963.

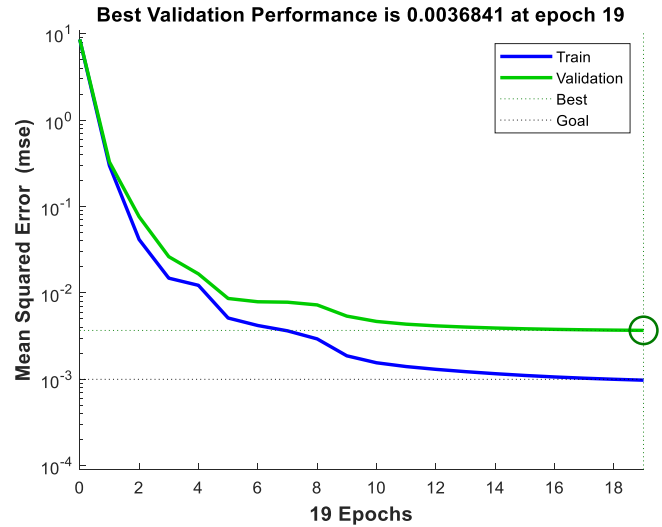
TABLE I  
 SPECIFIED AND ACHIEVED VALUES IN THE TRAINING AND VALIDATION PHASES OF THE ANN

ANN	Specified Values	Achieved Values
Iterations	100	19
Time (s)	60	2
Performance (MSE) Training	0.001	* 0.000858
Correlation ( $R^2$ )	1.0	0.9994
Performance (MSE) Validation	0.001	0.0036841
Correlation ( $R^2$ ) Validation	1.0	0.9963

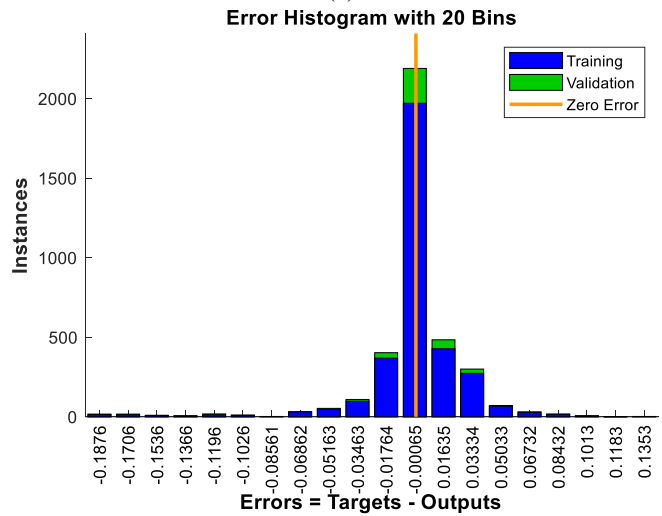
\* Achieved criterion.

Fig. 3(b) presents a histogram of the errors (difference between the obtained output ( $Y_{ob}$ ) and the desired output ( $Y_{des}$  = target)) with 20 intervals for the 1890 samples (2x1890 data points) during the training and validation phases. It is observed that the errors in both training and validation phases are close to zero, which explains the good performance shown in Fig. 3(a).

Fig. 4 presents the total real and reactive power losses for pre-contingency ( $r_0$ ) and all 20 contingencies ( $r_1, r_2, r_3, \dots, r_{20}$ ) of the IEEE 14-bus system, i.e., the desired ( $Y_{des}$ ) and obtained ( $Y_{ob}$ ) outputs in the two phases of the network (100% of the samples) as a function of the loading factor  $\lambda$ , the real and reactive power generated at the reference bus ( $P_g^{slack}$  and  $Q_g^{slack}$ ), and the branch number. A high similarity between the outputs is observed.



(a)



(b)

Fig. 3. Training and validation of the ANN, (a) performance (MSE), (b) error histogram ( $Y_{des} - Y_{ob}$ ) with 20 intervals for the 1890 samples.

The total real and reactive power losses for each phase of the ANN can be seen in Fig. 4. In the training phase, considered the most important part of the process, the network learns to provide responses based on the desired output (target to be followed), becoming capable of estimating data that were not part of the training. Fig. 4 illustrates the total real and reactive power losses for all 1890 samples, covering all system contingencies. In this analysis, we compare the desired output ( $Y_{des}$ ) with the obtained output ( $Y_{ob}$ ) using the Artificial Neural Network (ANN) in both the training and validation phases.

When observing the results, a remarkable correspondence between the desired and obtained outputs can be noted, highlighting the model's effectiveness in replicating the expected system behavior throughout the training process. This similarity indicates a high performance of the ANN, emphasizing its learning and generalization capabilities concerning the analyzed contingencies.

Fig. 5 presents only the samples used in the validation

phase, that is, those that were not part of the network's training. These results show that the ANN was able to accurately estimate the total real and reactive power losses by using only the input data provided, without any direct influence from the training dataset.

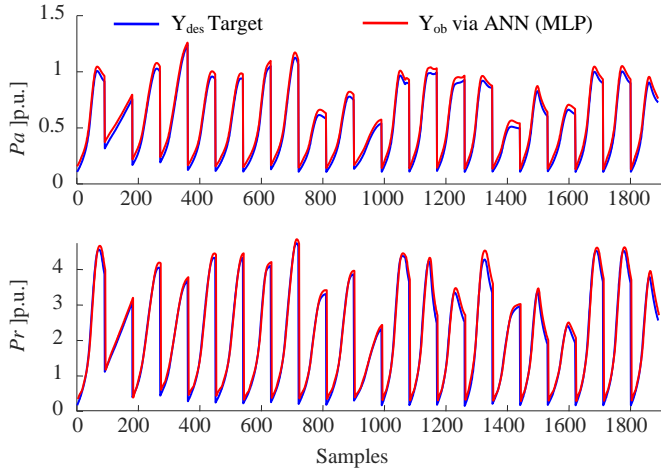


Fig. 4. Total real and reactive power losses ( $P_a$  and  $P_r$ ) for all applied contingencies (all 1890 samples), desired output ( $Y_{des}$ ) vs obtained output ( $Y_{ob}$ ) via ANN.

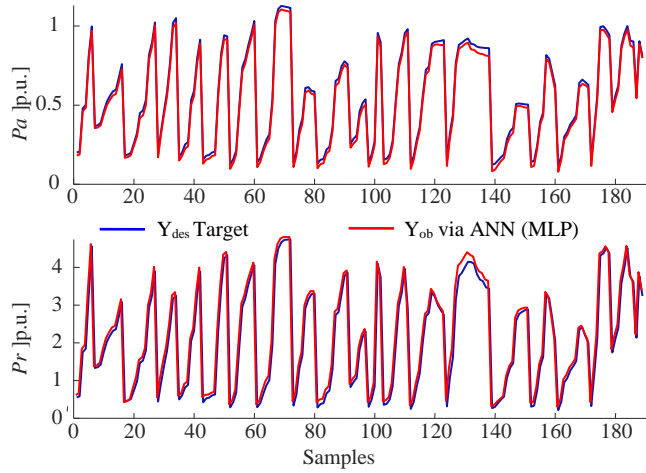


Fig. 5. Total real and reactive power losses ( $P_a$  and  $P_r$ ) for all applied contingencies (189 samples in the validation phase), desired output ( $Y_{des}$ ) vs obtained output ( $Y_{ob}$ ) via ANN.

Fig. 6 presents the total real power losses ( $P_a$ ) curves for all system contingencies as a function of the loading factor  $\lambda$ , showing the complete  $\lambda$ - $P_a$  curves. This analysis allows us to observe the correspondence between the desired outputs ( $Y_{des}$ ) and the outputs obtained ( $Y_{ob}$ ) by the Artificial Neural Network (ANN).

It is evident that the curves generated by the ANN closely follow the expected curves, highlighting the model's accuracy in capturing the relationship between the loading factor and active power losses across all system contingencies. The observed similarity confirms the effectiveness of the ANN in replicating the desired behavior, even under different operational conditions represented by the analyzed

contingencies. In the first plot of Fig. 6, two pre-contingency ( $N=0$  or  $r_0$ ) curves are presented. The blue line ( $Y_{des}$ ) represents the desired output obtained through conventional continuation power flow, while the red line ( $Y_{ob}$ ) shows the output obtained via the Artificial Neural Network (ANN).

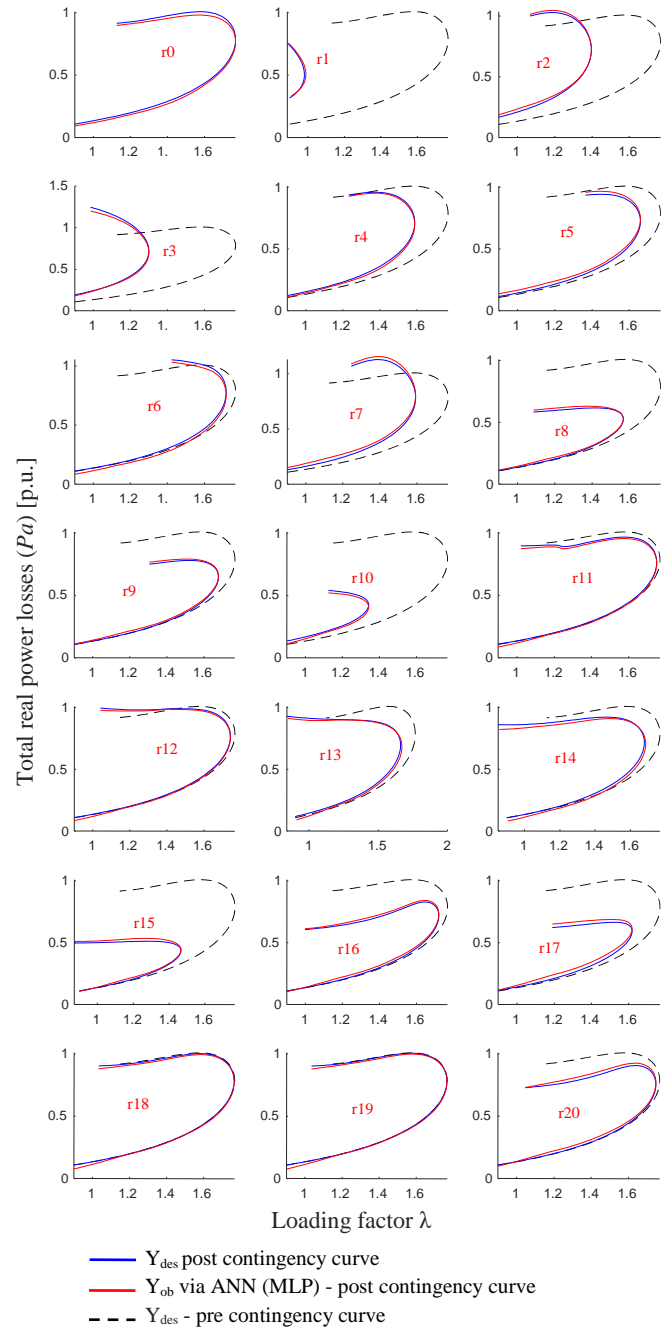


Fig. 6. Total real power losses ( $P_a$ ) for all applied contingencies (all 1890 samples), desired output ( $Y_{des}$ ) vs obtained output ( $Y_{ob}$ ) via ANN.

Fig. 7 shows the desired output for the total real power losses ( $P_a$ ) in relation to the contingency branches and the 90 points along the  $\lambda$ - $P_a$  curve. In contrast, Fig. 8 illustrates the output for  $P_a$  obtained via ANN, using the same parameters. It is noted that the difference between the desired results and those obtained by the ANN is virtually imperceptible.

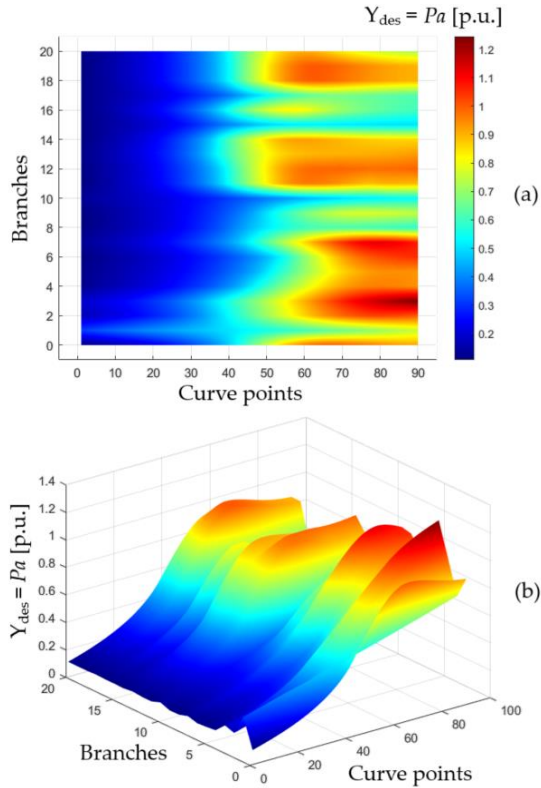


Fig 7. Desired  $Pa$  as a function of contingent branches and points, (a) 2D graph, (b) 3D graph.

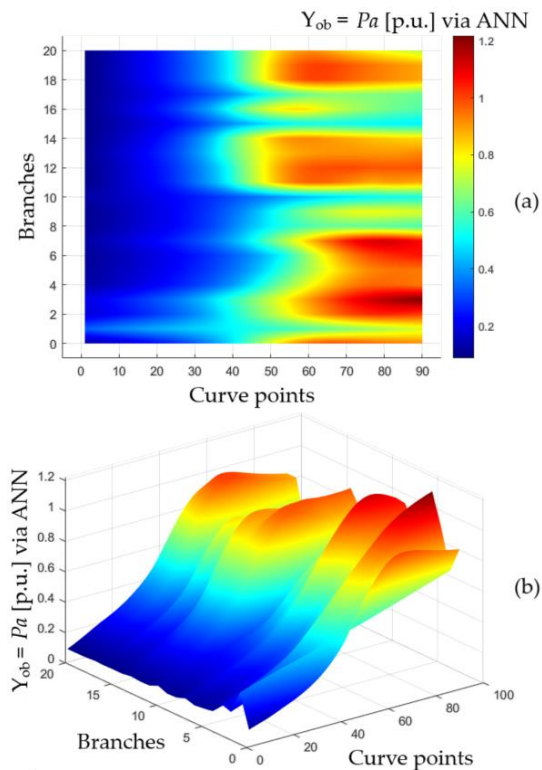


Fig 8.  $Pa$  obtained via ANN as a function of contingent branches and points, (a) 2D graph, (b) 3D graph.

Figure 9 presents the difference, or error, between the desired outputs and those obtained by the ANN for total real power losses ( $Pa$ ). It is observed that the error values are minimal, remaining close to zero. These results indicate that the neural network was able to replicate the desired outputs with great accuracy, demonstrating the model's effectiveness in predicting active power losses. The low magnitude of the errors reflects the robust performance of the ANN in the task, reinforcing its reliability as a modeling and forecasting tool.

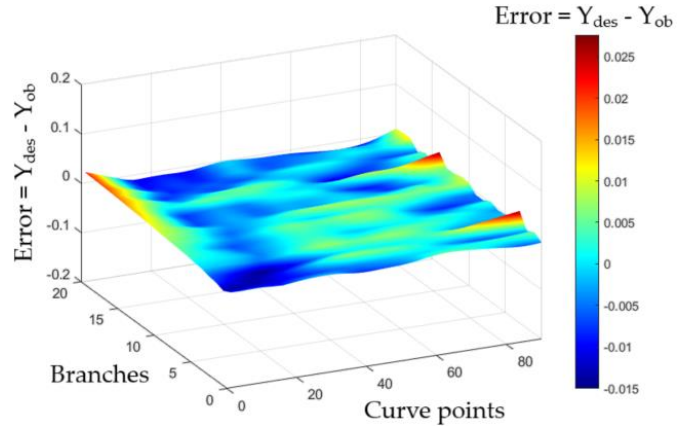


Fig 9. Desired output minus output obtained via ANN, i.e.  $Error = Y_{des} - Y_{ob}$  for total real power losses ( $Pa$ ).

Fig. 10 presents the total reactive power losses ( $Pr$ ) curves for all system contingencies as a function of the loading factor  $\lambda$ , showing the complete  $\lambda$ - $Pr$  curves. Examining the second plot related to contingency r1, three curves can be identified: one (dashed) represents the pre-contingency (N-0) curve for the loading factor  $\lambda$  versus reactive power ( $Pr$ ), while the other two curves correspond to the post-contingency conditions, representing the desired output (blue line -  $Y_{des}$ ) and the obtained output (red line -  $Y_{ob}$ ). Contingency r1 refers to the outage of the branch between buses 1 and 2 (N-2), as illustrated in Fig. 1.

A significant reduction in the loading margin is evident compared to the base case value, with the loading factor  $\lambda$  at the critical point (CP) of post-contingency reduced to 0.9810, as obtained by the Artificial Neural Network (ANN). This reduction reflects the ANN's ability to identify and quantify the impact of the contingency on the system's capacity.

Fig. 11 displays the desired output for total reactive power losses ( $Pr$ ) in relation to the contingency branches and the 90 points along the  $\lambda$ - $Pr$  curve. Conversely, Fig. 12 presents the output for  $Pr$  generated by the ANN, using the same parameters. It is also observed that the discrepancy between the expected results and those obtained by the ANN is almost non-existent.

Finally, Fig. 12 illustrates the error between the desired values ( $Y_{des}$ ) and the obtained values ( $Y_{ob}$ ) for total reactive power losses ( $Pr$ ). The analysis of this figure reveals a notable similarity between the predicted and desired outputs, highlighting the effectiveness and accuracy of the proposed model. These results, once again, reinforce the robustness of

the model and its ability to provide highly reliable predictions. The proximity of the error values to zero demonstrates that the model not only achieves high accuracy but also effectively replicates the expected patterns, solidifying its practical utility.

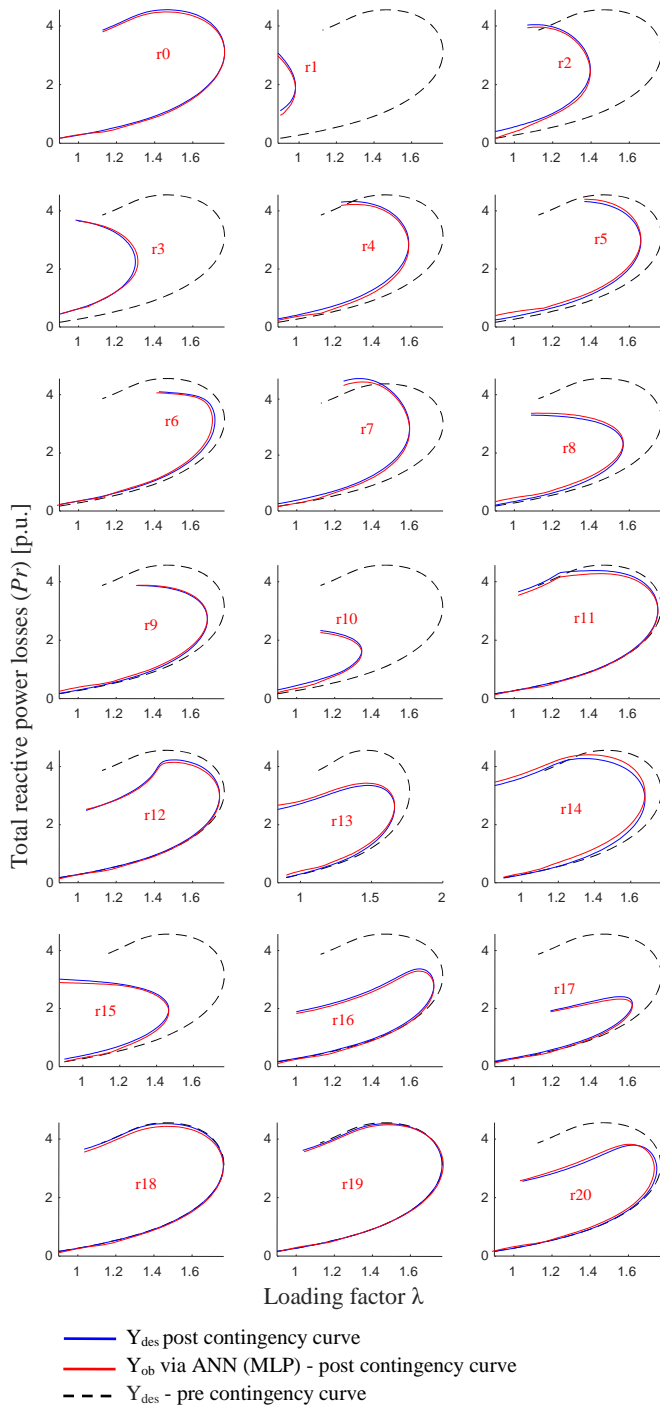


Fig. 10. Total reactive power losses ( $Pr$ ) for all applied contingencies (all 1890 samples), desired output ( $Y_{des}$ ) vs obtained output ( $Y_{ob}$ ) via ANN.

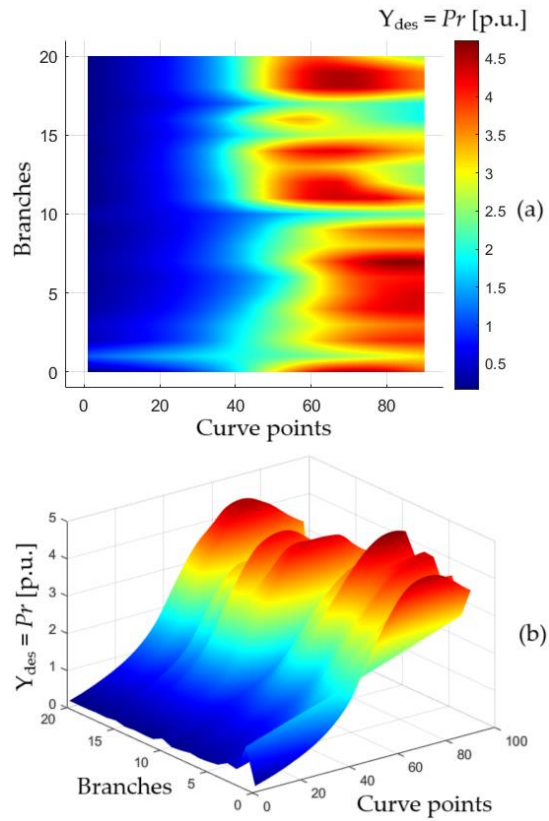


Fig 10. Desired  $Pr$  as a function of contingent branches and points, (a) 2D graph, (b) 3D graph.

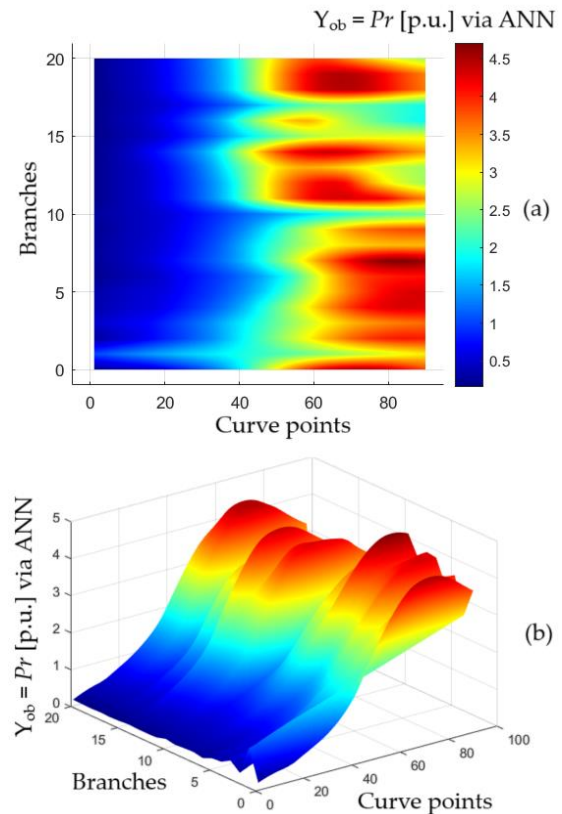


Fig 11.  $Pr$  obtained via ANN as a function of contingent branches and points, (a) 2D graph, (b) 3D graph.

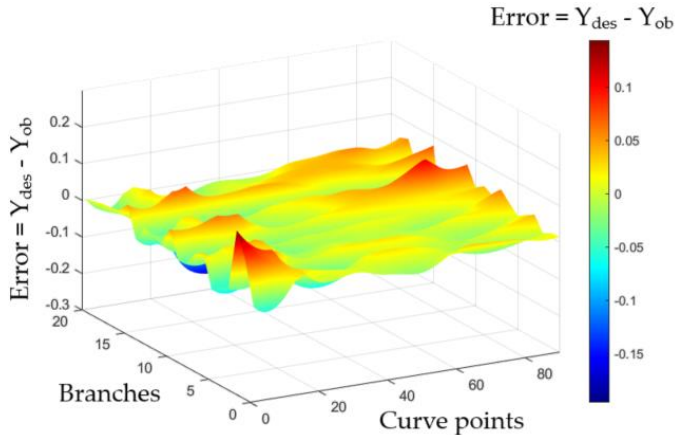


Fig 12. Desired output minus output obtained via ANN, i.e.  $Error = Y_{des} - Y_{ob}$  for total reactive power losses ( $Pr$ ).

## V. CONCLUSIONS

This work presented a methodology using Artificial Neural Networks (ANN) to determine the total real and reactive power losses, as well as to obtain the complete  $\lambda$ - $Pa$  and  $\lambda$ - $Pr$  curves of the power system subjected to contingencies, based on the loading factor  $\lambda$ , the real and reactive power generated at the reference bus ( $P_g^{slack}$  and  $Q_g^{slack}$ ), and the branch number. The results show that the neural network was well-trained, with a mean squared error (MSE) of 0.000858 at the nineteenth iteration, a training time of 2 seconds, and an  $R^2$  value for the training of 0.9994, indicating that the obtained output was quite close to the desired output. In the validation phase, for samples that did not participate in the training, the MSE obtained was 0.0036841, close to the specified limit of 0.001, resulting in a loading margin very close to the desired value. Overall, the ANN proved to be an efficient tool for determining energy losses.

## VI. ACKNOWLEDGMENT

The authors gratefully acknowledge the contributions of PROPG/Unesp, Coordenação de Aperfeiçoamento de Pessoal de Nível Superior - Brasil (CAPES) process n° 88887.956029/2024-00 and FAPESP – process 2023/03114-9.

## VII. REFERENCES

- [1] E. Bompard, T. Huang, Y. Wu, and M. Cremenescu. (2013). "Classification and trend analysis of threats origins to the security of power systems." *International Journal of Electrical Power & Energy Systems*, vol. 50, pp. 50-64.
- [2] Operador Nacional do Sistema Elétrico – ONS. PEN 2020. Sumário Executivo. Plano de Operação Energética 2020/2024. Disponível em: [http://www.ons.org.br/AcervoDigitalDocumentosEPublicacoes/ONS\\_PE\\_N2020\\_24\\_final%20\(6\).pdf](http://www.ons.org.br/AcervoDigitalDocumentosEPublicacoes/ONS_PE_N2020_24_final%20(6).pdf). Acesso em 17 jun. 2020.
- [3] R. R. Matarucco, A. Bonini Neto and D. A. Dilson. (2014). "Assessment of branch outage contingencies using the continuation method." *International Journal of Electrical Power & Energy Systems*, vol. 55, pp. 74-81.
- [4] W.P.L dos Santos, A. Bonini Neto and L.R.A Gabriel Filho. "Post-Contingency Loading Margin through Plane Change in the Continuation Power Flow." *Energies* 2023, 16, 7583. <https://doi.org/10.3390/en16227583>

- [5] M. Tostado-Véliz, S. Kamel and F. Jurado. (2020). "Development and Comparison of Efficient Newton-Like Methods for Voltage Stability Assessment." *Electric Power Components and Systems*, vol. 48, pp. 1798-1813.
- [6] A. Bonini Neto, J. C. Piazzentin and D.A. Alves. (2018). "Vandermonde Interpolating as Nonlinear Predictor Applied to Continuation Method." *IEEE Latin America Transactions*, vol. 16, no. 12, pp. 2954-2962.
- [7] Western System Coordinating Council (WSCC) (1998). Reactive Power Reserve Work Group. Final Report, Voltage Stability Criteria, Undervoltage Load Shedding Strategy, and Reactive Power Reserve Monitoring Methodology, May, 154p.
- [8] R. Zhang, Y. Xu, Z. Y. Dong, P. Zhang and K. P. Wong. (2013). "Voltage stability margin prediction by ensemble based extreme learning machine," *IEEE Power & Energy Society General Meeting*, pp. 1-5.
- [9] A. Gifalli, A. Bonini Neto, A. N. de Souza, R. P. de Mello, M. A. Ikeshoji, E. Garbelini, F. T. Neto. Fault Detection and Normal Operating Condition in Power Transformers via Pattern Recognition Artificial Neural Network. *Appl. Syst. Innov.* 2024, 7, 41. <https://doi.org/10.3390/asi7030041>
- [10] G. G. da Silva, A. de Queiroz, E. Garbelini, W. P. L. dos Santos, C. R. Minussi, A. Bonini Neto. Estimation of Total Real and Reactive Power Losses in Electrical Power Systems via Artificial Neural Network. *Appl. Syst. Innov.* 2024, 7, 46. <https://doi.org/10.3390/asi7030046>
- [11] A. Bonini Neto, D. A. Alves and C. R. Minussi. "Artificial Neural Networks: Multilayer Perceptron and Radial Basis to Obtain Post-Contingency Loading Margin in Electrical Power Systems." *Energies* 2022, vol. 15, 7939. <https://doi.org/10.3390/en15217939>
- [12] G. B. Huang, Q. Y. Zhu and C. K. Siew. (2006). "Extreme learning machine: theory and applications" in *Neurocomputing*, Vol. 70, No. 1, pp. 489–501.
- [13] F. Aydın and B. Gümüş. (2020). "Study of Different ANN Algorithms for Voltage Stability Analysis," in *Innovations in Intelligent Systems and Applications Conference (ASYU)*, pp. 1-5.
- [14] S. Haykin. (2008). *Neural networks and learning machines*, Prentice-Hall, 2008, 3rd. edition.
- [15] P.J. Werbos. (1974). "Beyond regression: new tools for prediction and analysis in the behavioral sciences", Ph.D. Thesis. Harvard University, Harvard.
- [16] Mathworks. Disponível em: <<http://www.mathworks.com>>. Acesso em: 02 de março de 2024.

## VIII. BIOGRAPHIES



**Giovana Gonçalves da Silva.** Degree in biosystems engineering from the São Paulo State University Júlio de Mesquita Filho - FCE -UNESP, Tupã (2021). Postgraduate degree in occupational safety engineering from UNIMAIS (2023). She is currently on a master's degree in electrical engineering at the São Paulo State University "Júlio de Mesquita Filho" - FEB - UNESP. She is a CAPES fellow in the development of the research project Intelligent systems and mathematical parameterization techniques applied to power flow. She received an honorary mention award for the best work presented at the XXXI CIC UNESP Tupã in 2019.



**Wesley Prado Leão dos Santos.** Graduating in Biosystems Engineering from São Paulo State University (Unesp), School of Sciences and Engineering, Tupã. He is currently a researcher in the area of electrical energy systems, with parameterization techniques and intelligent systems applied to continuation power flow.



**Alexandre de Queiroz.** Graduated in Data Processing Technology from the Faculty of Technology of Alta Noroeste in Araçatuba-SP in 2000. PhD student in the Postgraduate Program in Electrical Engineering, São Paulo State University (Unesp), School of Engineering, Bauru, working with Artificial Intelligence via graphical interface applied to predict parameters of electrical power systems. Computer programmer since 1992, the same year he completed the Technical Course in Data Processing integrated into High School. He presents knowledge and research in the area of artificial intelligence, with applications in various areas of knowledge



**Enio Garbelini.** Graduated in Mathematics from São Paulo State University (Unesp), School of Technology and Sciences, Presidente Prudente (1994), Master's degree in Applied Mathematics from the Federal University of Rio Grande do Sul (1999) and PhD in Electrical Engineering from São Paulo State University (Unesp), School of Engineering, Ilha Solteira. He is currently doing post-doctorate at São Paulo State University (Unesp), School of Sciences and Engineering, Tupã, with research in the area of artificial intelligence and parameterization techniques applied to continuation power flow.



**Alfredo Bonini Neto.** Degree in Mathematics (Licentiate) from the Faculty of Dracena - UNIFADRA (2002), and both a master's and doctorate in Electrical Engineering from the São Paulo State University Júlio de Mesquita Filho - FEIS - UNESP, Ilha Solteira (2006 and 2011). He completed his postdoctoral research in 2013 in Electrical Engineering at UNESP - Ilha Solteira, focusing on power systems and mathematical parameterization techniques for solving nonlinear equation systems, aiming at obtaining the critical point and eliminating the singularity of the Jacobian matrix. Currently, he is an Associate Professor at São Paulo State University - UNESP - Tupã Campus. His current research areas include Optimization, Continuation Methods (Parameterization Techniques), and Intelligent Computational Systems applied to Engineering, including Fuzzy Logic and Artificial Neural Networks.